

RESEARCH ARTICLE

Wind plant system engineering through optimization of layout and yaw control

Paul A. Fleming¹, Andrew Ning¹, Pieter M. O. Gebraad², Katherine Dykes¹

¹National Renewable Energy Laboratory (NREL)

²Delft Center for Systems and Control, Delft University of Technology

ABSTRACT

Recent research has demonstrated exciting potential for wind plant control systems to improve the cost of energy of wind plants. Wind plant controls seek to improve global wind plant performance over control systems in which each turbine optimizes only its individual performance by accounting for the way wind turbines interact through their wakes. While these technologies can be applied to existing wind plants, it is probable that the maximum benefit would be derived by designing wind plants with these capabilities in mind. In this paper, we use system engineering approaches to perform coupled wind plant controls and position layout optimizations of a model wind plant. We compare the result of this optimization, using several cost metrics, to the original plant, and as well to plants in which the control or layout is optimized separately, or optimized sequentially. Results demonstrate the benefit of this coupled optimization can be substantial, but depends on the particular constraints of the optimization.

Copyright © 0000 John Wiley & Sons, Ltd.

KEYWORDS

wind plant control; system engineering; wind turbine wakes; optimization

Correspondence

National Renewable Energy Laboratory (NREL), 15013 Denver West Parkway, Golden, CO 80401 . E-mail: paul.fleming@nrel.gov

Contract/grant sponsor

NREL's contributions to this work were supported by the U.S. Department of Energy under Contract No. DE-AC36-08GO28308 with the National Renewable Energy Laboratory.

Received . . .

1. INTRODUCTION

Wind turbines arranged in a cluster to form a wind plant, interact with each other through the wakes which they produce while extracting energy from the flow. This interaction, which has been studied thoroughly (see [1] for a literature overview), may have a negative effect on the total electrical power production of the wind plant. These effects can be mitigated by layout optimization, such as placing the turbines further away from each other, and/or by using wind plant control techniques during the operation of the plant, such as coordinating the control activities of individual turbines in order to increase power production for the plant as a whole.

Several approaches have been presented as methods for improving wind plant power capture. In one method, the power capture of upstream turbines is reduced in order to improve the performance, both in terms of power and loading, of downstream turbines. For some cases, even though the upstream turbines produce less power, the plant as a whole has a greater power output because of the downstream turbines' increased performance. This approach is evaluated in [2] and tested on a scaled model wind plant within a wind tunnel. Controllers making use of this effect are presented in [3–6]. Axial induction control is evaluated comparatively using models of varying fidelity, including computational fluid dynamics (CFD), in [7].

An alternative approach for using controls to improve global wind plant performance is to redirect the wake of upstream turbines to avoid interactions with downstream turbines. In [8], a CFD model is used to investigate the potential for turbines to redirect their wake laterally using yaw misalignment. In [9, 10], the Simulator for On/OffShore Wind Farm Applications (SOWFA), which is high-fidelity simulation tool that embeds wind turbine aero-servo-elastic models in a CFD flow, is used to investigate both the ability of turbines to redirect their wakes, as well as the production and loading impacts of doing so.

The yaw wake redirection method has been studied experimentally in wind tunnel tests with scaled turbines in [11] and [12]. Field tests with kW-scale turbines were performed in [13] with encouraging results, although the data was scattered yielding no clear conclusions. A correlation between yaw offset and a higher wind velocity downstream was demonstrated on a MW-scale turbine in [14].

Wind plant control algorithms, based on the results provided in the above literature review, have the potential to improve the power output of a wind plant by better coordinating the control activities of individual turbines. These technologies can be applied to existing wind plants, but it is probable that their benefit to wind plant production would be greatest for wind plants designed with these technologies in mind.

Traditional wind plant layout optimization has focused on maximizing energy production by placing turbines in the windiest locations while minimizing array losses due to wake effects. However, the state-of-the-art in plant design has extended to include a number of objectives including overall cost of energy that considers plant infrastructure and operations in addition to energy production and even non-economic objectives such as noise mitigation and minimization of environmental impacts. A recent work on the state of the art in wind plant optimization provides a comprehensive overview and examples of the various types of wind plant layout optimization studies that have been performed [15]. Generally, there is an increased recognition that coupling across the system requires more integrated approaches to wind plant design that consider a large range of decision criteria and more holistic approach to optimization. Systems engineering and multi-disciplinary analysis and optimization (MDAO) methods in particular hold promise for improving overall plant design for a range of system objectives [16].

However, the integration of wind plant controls with the design of a wind plant was not included in [15] though it has been treated at some level in past work. As an example, in [17], a multi-level optimization approach is used to optimize the layout of the Middelgrunden wind plant, in terms of maximizing wind plant profit with an overall cost of energy objective where turbine-level controls were an integral part of the study. Still, the active combination of wind plant controls for increased energy production or even reduced turbine loads has not been directly coupled to wind plant layout optimization in past studies.

In this paper, we use an engineering model of wake effects in a wind plant to consider the possibilities of combining wind plant controls with system-engineering-based layout optimization, and compare this coupled approach with the results from applying these methods separately. Specifically, for wind plant control we consider the technique of wake redirection through intentional yaw misalignment. For layout optimization, we use the wake model to find optimal wind plant layouts with and without wind plant control active. For this study, we model the Princess Amalia wind park in the Netherlands, to compare the performance of each technique.

The paper is intended as a proof-of-concept study on the combination of wind plant optimization techniques with wind plant controls. We use approximate means of estimating cost to allow this work to focus on the coupled optimization

methods prior to increasing the complexity. However, given the potential demonstrated by this coupled approach, future research will seek to refine the method to include more detailed models.

The contribution of this paper is an investigation into the potential for both wind plant control, and system-engineering approaches for improving wind energy performance. Additionally, the paper demonstrates how considering system design optimization and advanced control technologies simultaneously improves the design more than what is possible when applying either technique alone. This indicates that future wind plants might be designed considering the control systems which could be used to optimize plant-wide performance. Finally, we present analysis which indicates the relative importance of advanced controls versus layout optimization given the design constraints.

The remainder of this paper is organized as follows. In Section 2, we present the models we will use in the study. Section 3 presents the design cases to be considered, from separate control and layout optimizations, to coupled optimizations. In Section 4, detail is provided on the optimizations performed, including defining the cost function and constraints, as well as the optimization method used. The results of the optimizations are presented, analyzed and compared in Section 5. Finally, conclusions are given in Section 6.

2. WIND PLANT MODELS

2.1. Princess Amalia Wind Plant

As described in the introduction, we use as our test case the Princess Amalia Wind Plant, which is an offshore wind plant located 23 km off the coast of The Netherlands. The Princess Amalia Wind Plant consists of 60 wind turbines with a rotor diameter of 80 m and a rated power of 2 MW. The locations of the turbines in the Princess Amalia Wind Plant are shown in Figure 1. The spatial configuration of the turbines in the Princess Amalia Wind Plant is such that the wind turbines are further away from each other in the prevailing wind directions.

By using wind measurements at a nearby location, an estimate is made of the annual wind rose at the Princess Amalia Wind Park as shown in Figure 2. These wind measurements were made by the NoordzeeWind meteorological mast at a nearby location in the North Sea during the period from July 1st, 2005 to June 30th, 2006, [18].* The measurements consist of 10 minute averages of the wind direction and the free stream wind speeds and are available at [19]. In this study we focus only on the 8 m/s wind speeds and extract only this data. Note the wind rose data is binned into 5° increments, yielding 72 total bins.

From this data, we are able to develop an engineering model of the wind plant including wake interaction. Note however that the real wind plant is composed of Vestas V80 wind turbines with a rotor diameter of 80 m and a rated power of 2 MW, while for this exercise we employ NREL 5MW reference turbines (with rotor diameter of 126 m). This substitution is necessary because of the necessity for an open-access turbine model, which is available for NREL 5MW turbine. However, this substitution changes the effective spacing in terms of rotor diameters, and while we believe the comparison between optimization methods are still valid, the improvement relative to the baseline would probably be less given greater rotor diameter spacing.

2.2. FLORIS

In [10], the FLOW Redirection and Induction in Steady-state (FLORIS) model was presented, a control-oriented model that predicts the steady-state characteristics of wakes in a wind plant as a function of the axial inductions and yaw angles of the rotors. It is a static nonlinear model describing the velocity profile of the wakes (based on an augmented Jensen model, [20, 21]), and the wake deflection caused by yaw offset (based on the engineering model in [8]) and rotational effects. The augmentation to the Jensen model mainly consists of a segmentation of the wake in different zones such that

*The measurements are undisturbed by the NoordZeeWind offshore wind plant, that was constructed later.

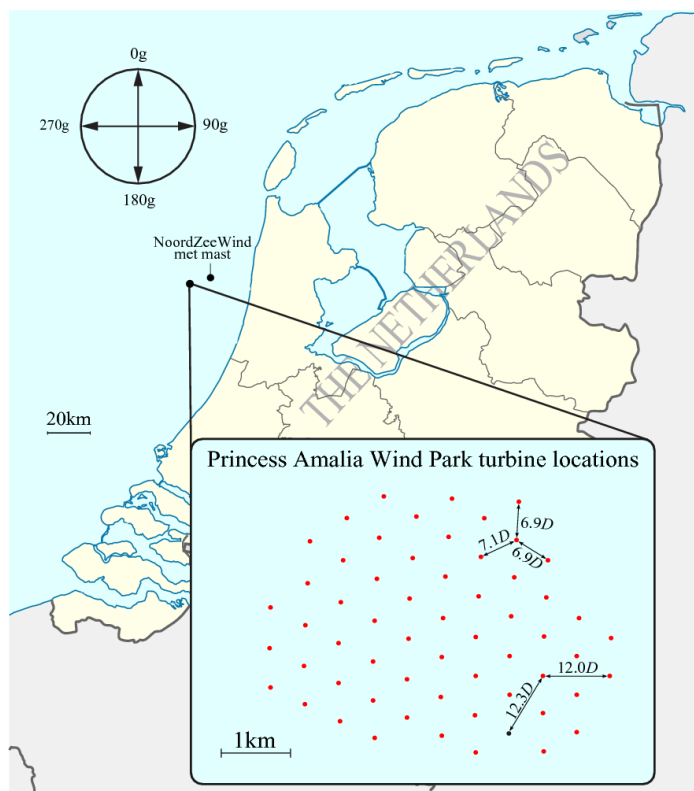


Figure 1. Lay-out and location of the Princess Amalia Wind Plant (source: [6]), the spacing between some of the turbine is shown with $D = 80$ m (the V80 rotor diameter).

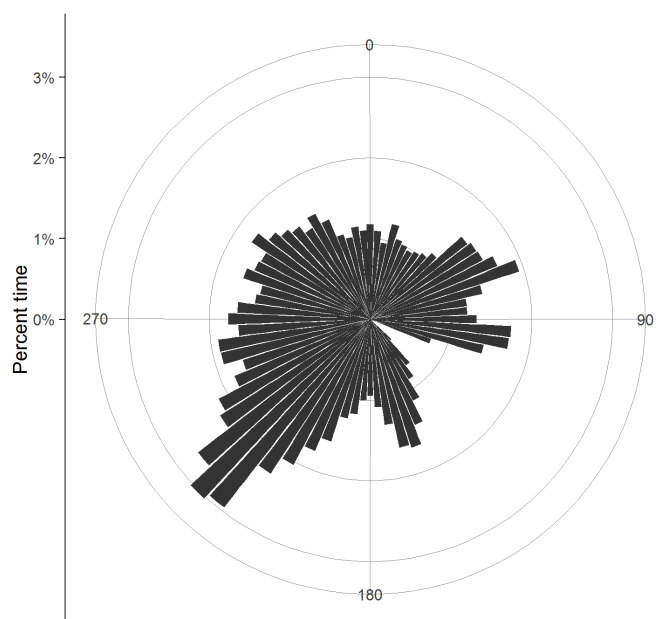


Figure 2. Estimated wind rose (in percentage) for Amalia wind plant, using wind data from the nearby NoordZeeWind met mast [19].

the cross-wind velocity profile of the wake can be better fitted. From the wake velocity profiles, the power of each of the wind turbines is estimated using the wake overlap weighting method described in [4].

While having a small amount of parameters to describe the relevant effects, the FLORIS model can be fit to the time-averaged results from high-fidelity simulations of situations with partial overlap of the turbine wakes with downstream rotors. The parameters were fit to the SOWFA simulation results [9] of a row of two NREL 5MW turbines, where the upstream turbine has a yaw offset or a cross-wind position offset. In [10] it was also shown that the predictions of the FLORIS model can be used to optimize the yaw angles of turbines in a wind plant for maximum power production.

3. PROBLEM DEFINITION

In the follow sections we investigate the opportunities for optimizing the wind plant using a FLORIS model of the Princess Amalia Wind Plant with NREL 5MW turbines. We consider layout optimization, optimized control (through yaw-based wake redirection), and finally a combined optimization of layout and control. This provides the following cases:

Baseline: fixed (original) positions, turbines all yawed in mean wind direction

Optimized yaw: fixed (original) positions, turbines optimally yawed for each wind direction

Optimized location: position optimized, turbines all yawed in mean wind direction

Combined optimization yaw optimized for each wind direction and position optimized simultaneously

The goal of wind plant optimization is to minimize the cost of energy (COE). The formula for COE is

$$\text{COE} = \frac{\text{FCR}(\text{TCC} + \text{BOS}) + \text{O\&M}}{\text{AEP}} \quad (1)$$

where FCR is the fixed charge rate, TCC, the turbine capital costs, BOS, the balance-of-station costs, O&M the operation and maintenance costs, and AEP the annual energy production.

The tradeoffs in balance-of-station costs versus annual energy production are site-specific, and in this paper we seek to explore solutions across a range of conditions. The relative cost, or even feasibility, of changing the overall shape of the wind plant will vary from site to site, as will the relative cabling costs. Rather than choose numbers for a specific site, we consider three surrogate metrics which capture tradeoffs in annual energy production versus balance-of-station and maintenance costs in different ways. While these metrics are not necessarily useful as absolute metrics, they are useful for comparing *relative* changes between layouts, which is the goal of this study. The first objective is to maximize the power density (or plant power / area). The second objective is to maximize power with a fixed total cabling length. The final objective is to maximize power with a fixed plant boundary. In all cases, minimum separation distances between turbines are enforced. For yaw-optimization, none of the costs are affected, and so a simple power maximization is sufficient.

The power used in the objectives, is an expected value of power across all wind directions, using the wind-speed-bin percentages shown in Figure 2. This averaging is done only at one wind speed (8 m/s). Area of the wind plant is computed as the area of the minimum-sized convex polygon using the outer-most turbines as vertices. Such a polygon is shown in Figure 3a. The polygon is computed using the SciPy scientific computing package for python [22]. Cable length is computed by finding the minimum spanning tree for the given layout. The minimum spanning tree is the set of lines which connect all the turbines in a single graph with minimal total length of lines. The minimum spanning tree is computed using an implementation of Prim's algorithm [23]. The cable length for the baseline layout is shown in Figure 3b.

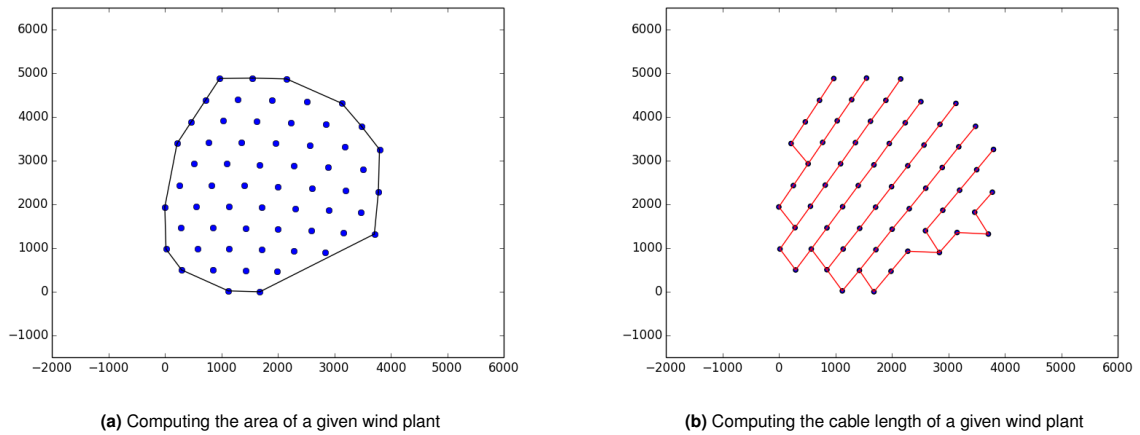


Figure 3. Computing area and cable length of a given wind plant layout.

4. OPTIMIZATION

In this paper, we consider the maximal benefit for the model wind plant by optimizing control, layout, or a combination of both. In this section, we provide detail on the optimization routine employed, as well as the specific optimizations carried out for each case.

All optimizations in this paper were performed using the software package SNOPT [24], a nonlinear optimization package based on the sequential quadratic programming method. The pyOpt wrapper [25] was used to call SNOPT from Python. Gradients were estimated using finite differencing, and all results were converged with an optimality tolerance of 5×10^{-5} and a feasibility tolerance of 1×10^{-6} . Objectives and constraints were normalized to be of order one.

In the baseline case, all the metrics (mean power, area, cable length) are computed assuming that for each wind direction, the turbines are yawed into the wind, and the positions of the turbines are from the originally provided layout.

4.1. Yaw Optimization (Control Only)

For each wind direction, the yaw angle of each turbine was optimized to maximize power production. Because yaw control is assumed, the optimizations for each wind direction are independent. This leads to 72 (one for each wind direction bin) optimization problems of the form:

$$\begin{aligned}
 &\underset{\psi}{\text{maximize}} && P(x, y, \psi)_i \\
 &\text{subject to} && -\pi/4 \leq \psi \leq \pi/4
 \end{aligned} \tag{2}$$

Where x and y are the (fixed) turbine locations and ψ are the turbine yaw angles. The bound constraints on yaw angle were used to prevent exploitation of unphysical solutions that sometimes arise in this model for highly yawed solutions. This optimization problem will be referred to as *YawOpt*.

4.2. Position Optimization (Layout only)

For all three position optimization applications, the position of the wind turbine affects the power production for all wind directions, and so evaluation across the complete wind rose must be done at each iteration. The x and y locations of the wind turbines were included as design variables. However, if all x , y variables were included then there would be no unique solutions. Because there are no domain boundaries, the entire array of turbines could be shifted an arbitrary amount in any direction and the power output would remain unchanged. To prevent this non-uniqueness, the position of the last turbine at

location: (1683.7, 0.0) remain fixed. All other positions were added as design variables. For convenience, the specification of the optimization problems in the below sections uses x, y to represent the vector of all turbines positions, excepting the last turbine. In the optimization all positions were normalized by 1000, and to prevent unrealistic intermediate solutions the positions were constrained to stay within a box of half-width 1.0 (or 1000 in physical coordinates) from their starting point.

The inter-turbine spacing constraint constrains the distance from each turbine with every other turbine to be greater than 2 diameters. This results in $(n^2 - n)/2$ spacing constraints (1,770). This constraint is expressed below as $d_i \geq 2D$, $i = 0 \dots 1,770$.

We now define the three separate layout position optimization cases, each one will be indicated by $PosOpt$, with a specifying suffix.

4.2.1. Case: $PosOpt_{Density}$

Case $PosOpt_{Density}$ maximizes power density (expected power/area), with a constraint on minimum expected power generation and a minimum turbine separation distance. A constraint on the minimum expected power production is added to prevent the optimizer from driving the solution to unrealistically small areas. The tradeoff in area and power production is such that it is generally easier to decrease area than it is to increase power production. Thus, maximizing power density often results in spacings that are too dense, even with the minimum spacing constraint. Adding the minimum power constraint prevents that behavior. The new layout must produce at least as much power as the original layout. Lastly, note that in the position-optimized cases, it is assumed that wind turbine yaw controllers operate normally, and so ψ is always chosen to be aligned with the inflow wind direction for all turbines.

$$\begin{aligned}
 &\underset{x,y}{\text{minimize}} && E[P](x, y, \psi)/A \\
 &\text{subject to} && E[P] \geq E[P]_0 \\
 &&& d_i \geq 2D, \quad i = 0 \dots 1,770 \\
 &&& x_{i0} - 1000 \leq x_i \leq x_{i0} + 1000, \quad i = 0 \dots 59 \\
 &&& y_{i0} - 1000 \leq y_i \leq y_{i0} + 1000, \quad i = 0 \dots 59
 \end{aligned} \tag{3}$$

4.2.2. Case: $PosOpt_{Cable}$

Case $PosOpt_{Cable}$ maximizes the expected power with a constraint on the maximum cable length. The total cabling length between all the turbines is computed as l , and is enforced to be no greater than the original total cabling length l_0 . The optimization problem is summarized as:

$$\begin{aligned}
 &\underset{x,y}{\text{minimize}} && E[P](x, y, \psi) \\
 &\text{subject to} && l \leq l_0 \\
 &&& d_i \geq 2D, \quad i = 0 \dots 1,770 \\
 &&& x_{i0} - 1000 \leq x_i \leq x_{i0} + 1000, \quad i = 0 \dots 59 \\
 &&& y_{i0} - 1000 \leq y_i \leq y_{i0} + 1000, \quad i = 0 \dots 59
 \end{aligned} \tag{4}$$

4.2.3. Case: $PosOpt_{Boundary}$

Case $PosOpt_{Boundary}$ maximizes the expected power with a fixed original boundary. The closest normal distance from every turbine to the boundary is computed and stored in n_i . If n_i is negative it means the turbine is within the boundary. The optimization problem is given as:

$$\begin{aligned}
& \underset{x,y}{\text{minimize}} && E[P](x, y, \psi) \\
& \text{subject to} && n_i \leq 0, \quad i = 0 \dots 59 \\
& && d_i \geq 2D, \quad i = 0 \dots 1,770 \\
& && x_{i0} - 1000 \leq x_i \leq x_{i0} + 1000, \quad i = 0 \dots 59 \\
& && y_{i0} - 1000 \leq y_i \leq y_{i0} + 1000, \quad i = 0 \dots 59
\end{aligned} \tag{5}$$

4.3. Yaw and Position Optimization

This final scenario consists of optimizing the positions of the turbines and the yaw angles of all the turbines at each wind direction simultaneously (4,438 total design variables). The combined position and yaw optimization problem is posed as a monolithic optimization problem rather than a nested problem. Even though the yaw angles can be independently chosen at each wind direction, it was deemed that finite differencing across an internal optimization problem would be less effective. Also, while the monolithic problem has a large number of design variables, the vast majority of the computational cost is in computing the finite differences and that is easily parallelized. For this problem we use 192 cores, and a run time of 36 hours, and make use of pyOpt's ability to do finite differencing in a parallel manner. The optimization problem is stated below, where capital Ψ is used to denote the concatenation of all the yaw vectors (lower case ψ) across all wind directions. All three cases for the position optimization are explored as a combined position/yaw optimization. These cases will be identified as YP . As above, the separate cases are identified by the subscripts: density, cable, and boundary.

$$\begin{aligned}
& \underset{x,y,\Psi}{\text{minimize}} && E[P](x, y, \Psi) \\
& \text{subject to} && \text{minimum power, maximum cabling length, or fixed boundary} \\
& && d_i \geq 2D, \quad i = 0 \dots 1,770 \\
& && x_{i0} - 1000 \leq x_i \leq x_{i0} + 1000, \quad i = 0 \dots 59 \\
& && y_{i0} - 1000 \leq y_i \leq y_{i0} + 1000, \quad i = 0 \dots 59 \\
& && -\pi/4 \leq \Psi \leq \pi/4
\end{aligned} \tag{6}$$

Because of the large number of design variables obtaining the same tight convergence tolerances requires exponentially longer compute times. Instead, the objective function was monitored until no discernable changes were observed. Figure 4 shows the objective function for each combined position/yaw optimization against the iteration step, showing that with this level of computation, the solution seems to have converged.

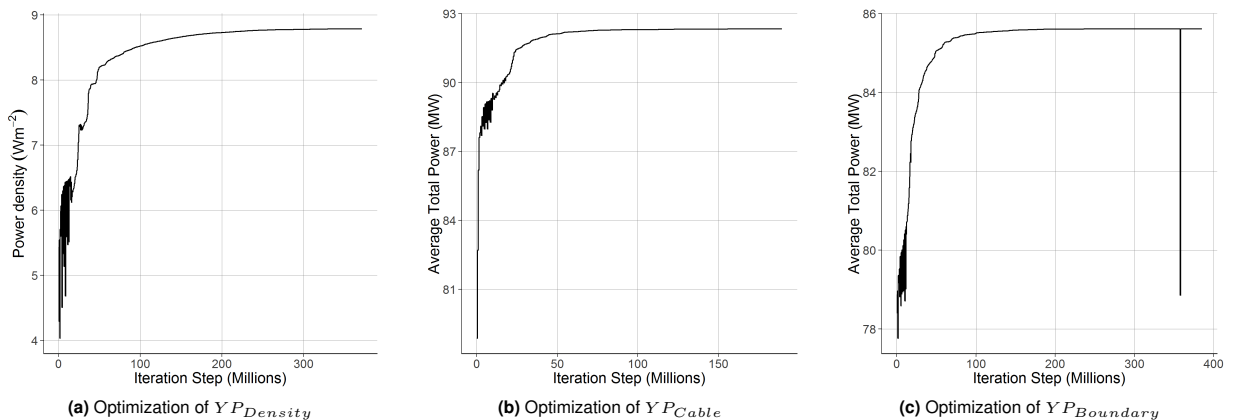


Figure 4. Optimization objection plotted against iteration step.

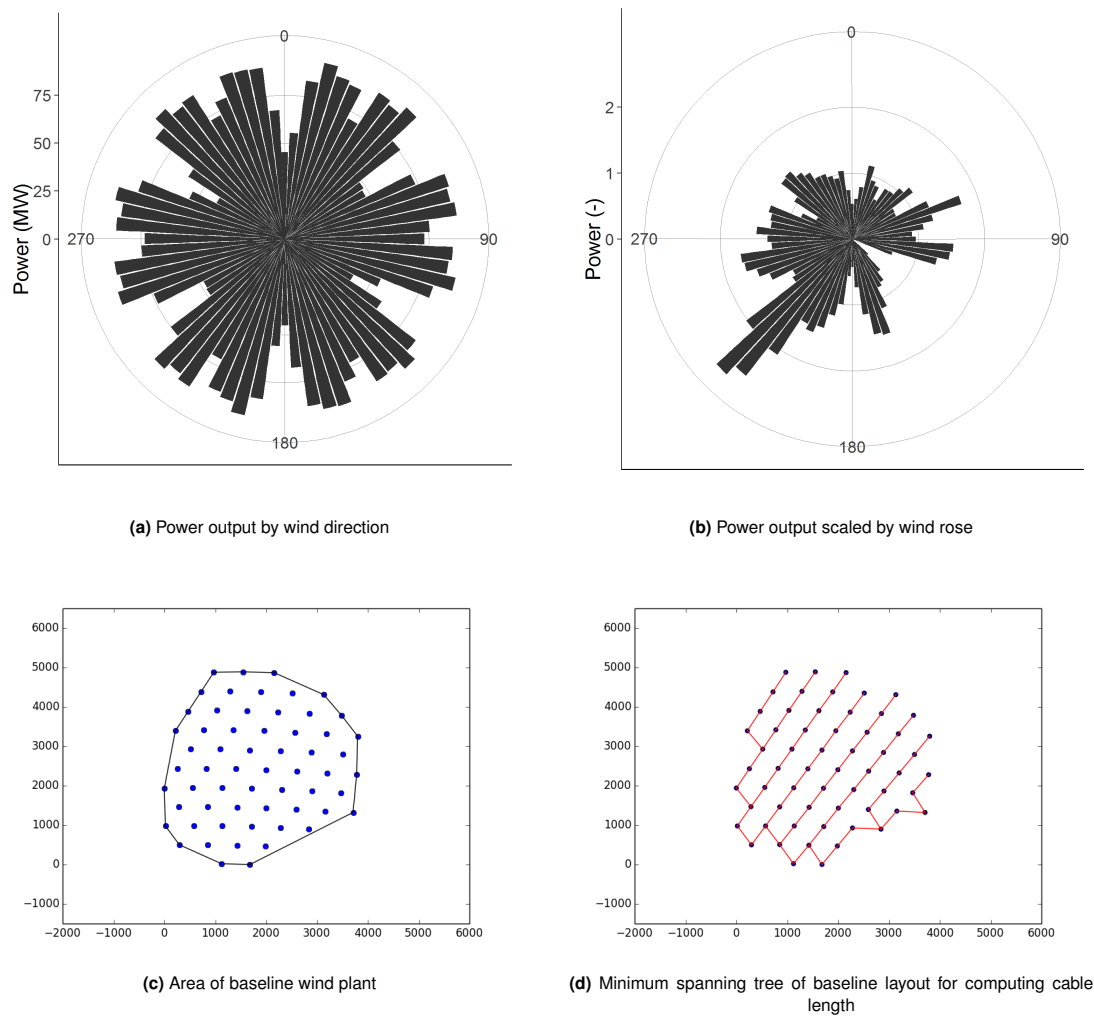


Figure 5. Power output and layout cost functions for the Baseline case.

Table I. Key metrics of the Baseline case.

	<i>Baseline</i>
Mean Power (MW)	78.86
Area (km ²)	14.53
Cable Length (km)	32.74
Power Density (W/m ²)	5.43

5. RESULTS

Having defined the optimization problems, we now review the results for each case. First we present the analysis of the baseline case.

5.1. Baseline

The baseline case has the turbines positioned according to their original layout, and for each wind direction each turbine is yawed into the wind. In Figure 5, the results of the baseline analysis are shown.

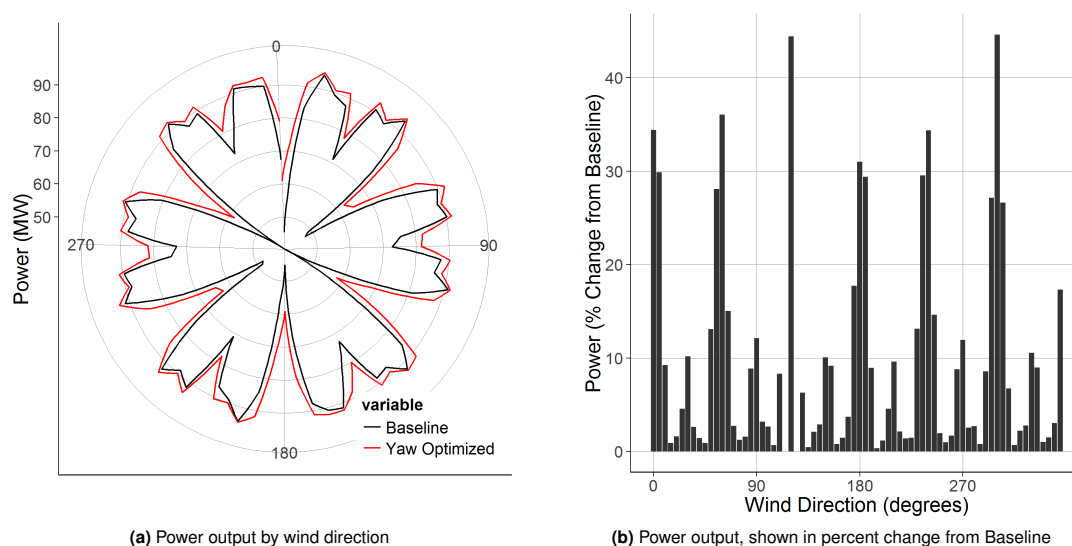


Figure 6. Yaw-optimized power performance plots

Table II. Key metrics of the YawOpt case.

	<i>Baseline</i>	<i>YawOpt</i>
Mean Power (MW)	78.86	84.91
Area (km ²)	14.53	14.53
Cable Length (km)	32.74	32.74
Power Density (W/m ²)	5.43	5.84

Figure 5a shows the power output of the baseline wind plant for each wind direction. It can be seen that in those directions in which the wind is aligned with the wind plant rows correspond to significant reductions in power output. This is caused by the wake effects, which decrease power production for the turbines behind the lead row. In Figure 5b, the power is re-plotted after scaling by the wind rose, shown in Figure 2. Figure 5c shows the layout of the baseline wind plant, and the bounding polygon used to compute the area. The minimum spanning tree is shown in Figure 5d, to indicate the length of cable required in the baseline case. Finally, Table I indicates the values of the key metrics: mean power production, area, cable length and power density.

5.2. Yaw-optimized

Figure 6 considers the control-only case (yaw-optimized). Figure 6a shows the power output of this case for each wind direction, against the values from the Baseline case. Note that power production is increased for every wind direction. Figure 6b shows the percent change in power, relative to the baseline, for each wind direction. These plots show that the yaw control improves the power performance of each wind direction, most especially in the directions for which wake losses are greatest. Yaw control of course does not impact the layout of the wind plant, and so plots for area and cabling length are unaffected and not shown. Looking now at the Table II, it can be seen that overall, yaw control increases the mean power output (and likewise power density) by 7.7%.

5.3. Position Optimization

As discussed in Section 4.2 there are three different objectives explored for position optimization. $PosOpt_{Density}$ seeks to maximize power density (power/area) while constraining the power production to be greater than or equal to the baseline power production. $PosOpt_{Cable}$ seeks to maximize power output while constraining the cable length to be less than or

equal to the baseline length. $PosOpt_{Boundary}$ assumes the original boundary of the wind plant is fixed and seeks to maximize power output within that boundary. The results of the three optimizations are summarized in Figure 7.

For $PosOpt_{Density}$, Figure 7 shows that the optimization succeeds in increasing the power density. Considering Figure 7c and Table III, it can be seen that this is achieved through shrinking the plant area while maintaining the mean power output, as expected. Note that in Figure 7c, the original boundary of the wind plant is shown by the black dashed line. Interestingly, the wind plant is rearranged into a more streamlined shape. In the primary wind direction (from the southwest), the wind turbines are staggered so that wake effects are reduced on the downstream wind turbines. Further, few wind turbines are used in the front, while in the back they are packed together to extract as much momentum as possible because there are no downstream turbines to experience negative wake effects. In the least probably wind direction, the turbines remain in grid lines. The most probable and least probable wind directions are almost 90 degrees apart for this wind site.

$PosOpt_{Cable}$ works at spacing the turbines as far apart as possible, to minimize wake effects, while still maintaining a constant cable length (Figure 7g). This allows for much greater power capture. The wind plant has aligned itself into what are essentially 5 rows facing the predominant wind direction, but spaced them out as far as possible while keeping a few wind turbines between the rows to maintain the cabling length.

Finally the results of $PosOpt_{Boundary}$ are shown in Figure 7e. This optimization is restricted to the original boundary so there is less flexibility. The turbines are pushed toward the outer boundary to create as much spacing as possible, and turbines are staggered in the predominant wind direction, both of these changes reduce wake losses and increase power production as compared to the baseline design.

Each optimization succeeds in finding a new layout that has better performance, for the metric it seeks to optimize, as compared to the baseline, as shown in Table III. In comparing just $PosOpt_{Boundary}$ and Yaw-Opt, we see that control optimization, rather than layout optimization, was more effective in increasing mean power for a fixed original boundary.

5.4. Combined optimization

In the final set of optimizations, we consider optimizations which combine yaw-control optimization and position layout optimization, (signified by YP). These results are summarized in Figure 8.

Reviewing Table IV, it can be seen that the combined optimizations are superior to either the control-only or the layout-only optimizations for each case. $YP_{Density}$, achieves a significantly smaller plant area as compared to $PosOpt_{Density}$, while still maintaining approximate equivalent mean power. This results in a nearly 40% increase in power density as compared to optimizing position alone. It appears that for tightly spaced wind plants, the effect of yaw control is especially important in increasing power density. When comparing $PosOpt_{Cable}$ and YP_{Cable} we see that adding yaw optimization to the position optimization also result in an improvement, but the improvement was a much smaller increase in mean power (2%). For plants which are less constrained by area and can increase spacing, the position optimization appears to be more effective than the yaw-control optimization. Finally, for a fixed area, comparing $YawOpt$, $PosOpt_{Boundary}$, and $YP_{Boundary}$, it appears as if the effect of yaw-control is much more important. Of the potential 8.5% in total improvement due to optimizing yaw and position simultaneously, yaw-control alone can achieve 85% of the same benefit, whereas position optimization alone can only achieve 27% of the potential benefit.

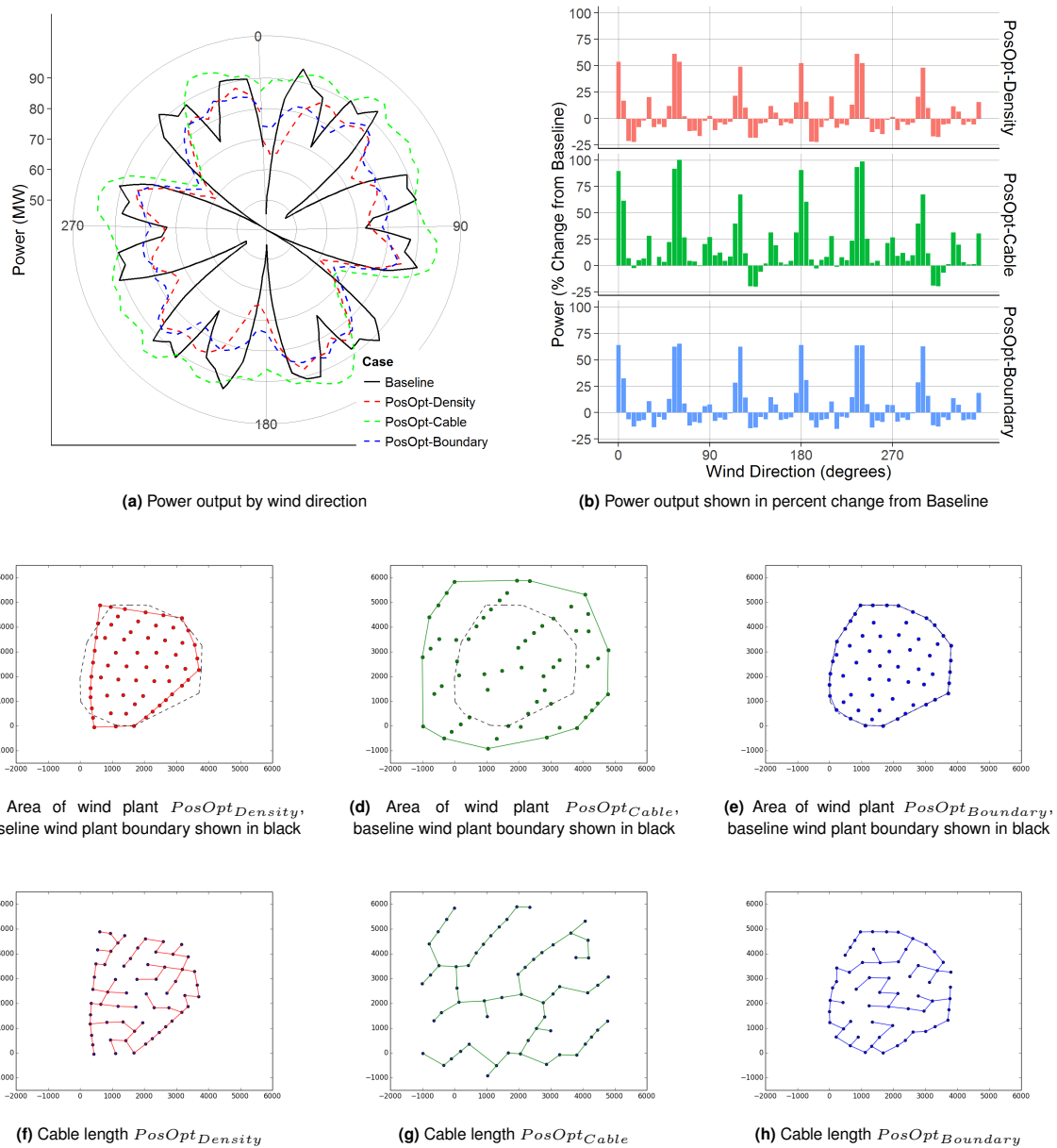
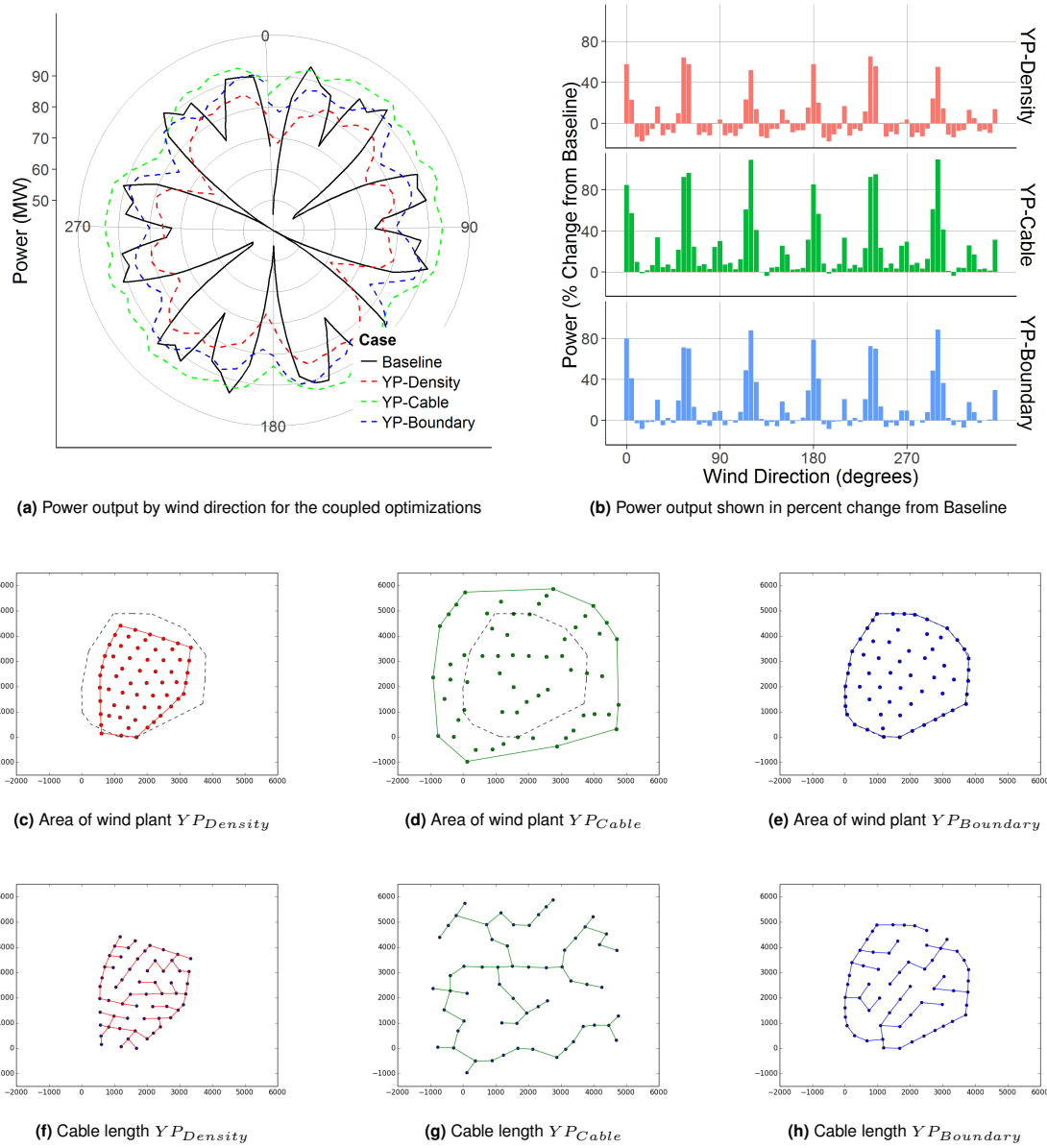


Figure 7. Results of power performance, area and cable length for position optimized cases

Table III. Comparison of Baseline, YawOpt and PosOpt key metrics.

	<i>Baseline</i>	<i>YawOpt</i>	<i>PosOpt_{Density}</i>	<i>PosOpt_{Cable}</i>	<i>PosOpt_{Boundary}</i>
Mean Power (MW)	78.86	84.91	78.86	90.67	80.68
Area (km ²)	14.53	14.53	12.45	33.28	14.47
Cable Length (km)	32.74	32.74	27.50	32.74	28.45
Power Density (W/m ²)	5.43	5.84	6.33	2.72	5.58

**Figure 8.** Results for yaw control and layout position coupled optimized cases**Table IV.** Comparison of Baseline, YawOpt, PosOpt, and YP key metrics.

	<i>Baseline</i>	<i>YawOpt</i>	<i>PosOpt_{Density}</i>	<i>PosOpt_{Cable}</i>	<i>PosOpt_{Boundary}</i>	<i>YP_{Density}</i>	<i>YP_{Cable}</i>	<i>YP_{Boundary}</i>
Mean Power (MW)	78.86	84.91	78.86	90.67	80.68	78.84	92.33	85.61
Area (km ²)	14.53	14.53	12.45	33.28	14.47	8.96	32.53	14.48
Cable Length (km)	32.74	32.74	27.50	32.74	28.45	23.88	32.74	27.80
Power Density (W/m ²)	5.43	5.84	6.33	2.72	5.58	8.80	2.84	5.91

5.5. Sequential optimization

It is expected that an integrated optimization approach will be more effective than a sequential one in which the layout is optimized first and then yaw angles are optimized afterwards for the new fixed layout. However, it is not obvious how significant the improvement is from combined optimization, and whether or not the increased complexity is warranted. We compared all three combined yaw-position optimization cases to a sequential approach where the layout was first optimized, and then the yaw angles were optimized following the selection of the optimal layout. These three sequential optimizations are denoted as SeqOpt, and a comparison of the results is shown in Table V.

Reviewing the results, for the density layout optimizations ($SeqOpt_{Density}$ and $YP_{Density}$), it can be seen that the coupled optimization was far more successful at maximizing power density, than the sequential. Conversely, the cable-length optimizations saw only a minor difference in performance (it would appear that $YPCable$ is not fully converged as it should be higher than $SeqOpt_{Cable}$, however the difference appears to be negligible so tightening the convergence will not yield additional insight.) The difference is related to the relative importance of considering control. The density optimizations are attempting to contract the layout of the park, which decreases turbine spacing, magnifying the importance of control in the optimization. The cable optimizations expand the layout, and therefore obtain much less impact from control, and therefore whether or not control is included in the layout optimization is much less important. Finally, in considering the boundary optimizations, there is shown here some benefit to including control in the layout optimization, but the difference between the two results is not large (0.5%).

6. CONCLUSIONS

This paper presented the results for several optimizations of a model wind plant, control-based, position (layout)-based, and then coupled optimizations of control and position (both simultaneous and sequential). Reviewing the presented results, it is shown that the best overall improvement was achieved by the coupled control and position optimizations.

The three layout scenarios (density, cable and boundary) each provide an instructive set of results on the possibilities for optimization, and the relative importance of control versus position layout, as well as the importance of simultaneous versus sequential optimization. The density cases, in which the optimization is seeking to make the plant as small as possible, require full simultaneous coupling to achieve optimal results: the power density of $YP_{Density}$ is 28.7% greater than $SeqOpt_{Density}$, and 31% greater than $PosOpt_{Density}$. The boundary cases, which have a fixed area, demonstrate overall optimal performance for the simultaneous coupled optimization $YP_{Boundary}$, however, the cases which include control, $YP_{Boundary}$ and $SeqOpt_{Boundary}$, are not a substantial improvement over yaw control alone (0.8% and 0.3% respectively), suggesting in this case control is primarily important and only minimal gain can be achieved with position optimization, regardless of coupling to control. Finally, the cable length cases, which expand the wind farm, appear now to be dominated by the position optimization. Additional improvement still is achieved by applying control (1.8%),

Table V. Comparing Seq-Opt and YP-Opt

	$SeqOpt_{Density}$	$SeqOpt_{Cable}$	$SeqOpt_{Boundary}$	$YP_{Density}$	$YPCable$	$YP_{Boundary}$
Mean Power (MW)	84.12	92.91	85.14	78.84	92.33	85.61
Area (km ²)	12.45	33.28	14.47	8.96	32.53	14.48
Cable Length (km)	27.50	32.74	28.45	23.88	32.74	27.80
Power Density (W/m ²)	6.84	2.72	5.88	8.80	2.84	5.91

however in this case, simultaneous optimization of control and position appears to add negligible benefit over a sequential optimization.

It is important to again note that this study is focused on the method for optimizing wind plant controls and layout optimization and so as discussed, a number of simplifications were employed to avoid over-complicating a first study. A real wind plant design could include many further constraints on layout (given realities such as topography or zoning regulations). Future work will expand on these initial results to include more realistic constraints and fuller definitions of cost of energy.

REFERENCES

1. Sanderse B, van der Pijl S, Koren B. Review of computational fluid dynamics for wind turbine wake aerodynamics. *Wind Energy* 2011; **14**(7):799–819.
2. Corten G, Schaak P. Heat and flux: Increase of wind farm production by reduction of the axial induction. *European Wind Energy Conference*, Madrid, Spain, 2013.
3. Johnson KE, Thomas N. Wind farm control: addressing the aerodynamic interaction among wind turbines. *American Control Conference*, IEEE, 2009; 2104–2109.
4. Marden JR, Ruben S, Pao L. A model-free approach to wind farm control using game theoretic methods. *IEEE Transactions on Control Systems Technology* 2013; .
5. Soleimanzadeh M, Wisniewski R, Johnson K. A distributed optimization framework for wind farms. *Journal of Wind Engineering and Industrial Aerodynamics* 2013; **123**:88–98.
6. Gebraad PMO, van Wingerden JW. Maximum power-point tracking control for wind farms. *Wind Energy* 2014; .
7. Annoni J, Seiler P, Johnson K, Fleming P, Gebraad P. Evaluating wake models for wind farm control. *Proceedings of the American Control Conference*, Portland, OR, USA, 2014.
8. Jiménez Á, Crespo A, Migoya E. Application of a LES technique to characterize the wake deflection of a wind turbine in yaw. *Wind energy* 2010; **13**(6):559–572.
9. Fleming PA, Gebraad PM, Lee S, van Wingerden JW, Johnson K, Churchfield M, Michalakes J, Spalart P, Moriarty P. Evaluating techniques for redirecting turbine wakes using sowfa. *Renewable Energy* 2014; .
10. Gebraad PMO, Teeuwisse FW, van Wingerden JW, Fleming PA, Ruben SD, Marden JR, Pao LY. A data-driven model for wind plant power optimization by yaw control. *Proceedings of the American Control Conference*, Portland, OR, USA, 2014. URL <http://bit.ly/11528md>.
11. Adaramola MS, Krogstad PÅ. Experimental investigation of wake effects on wind turbine performance. *Renewable Energy* 2011; **36**(8):2078–2086.
12. Medici D. Experimental studies of wind turbine wakes: power optimisation and meandering. PhD Thesis, KTH Royal Institute of Technology 2005.
13. Wagenaar J, Machielse L, Schepers J. Controlling wind in ECN's scaled wind farm. *Proceedings of EWEA*, Copenhagen, Denmark, 2012.
14. Soleimanzadeh M, Wisniewski R, Brand A. State-space representation of the wind flow model in wind farms. *Wind Energy* 2014; **17**(4):627–639.
15. Herbert-Acero JF, Probst O, Réthoré PE, Larsen GC, Castillo-Villar KK. A review of the state of the art in wind farm optimization. *Energies* 2014; **7**.
16. Dykes K, Meadows R, Felker F, Graf P, Hand M, Lunacek M, Michalakes J, Moriarty P, Musial W, Veers P. *Applications of systems engineering to the research, design, and development of wind energy systems*. National Renewable Energy Laboratory, 2011.
17. Réthoré PE, Fuglsang P, Larsen GC, Buhl T, Larsen TJ, Madsen HA. Topfarm: Multi-fidelity optimization of offshore wind farm. *Proceedings of the Twenty-first International Offshore and Polar Engineering Conference*, Maui, Hawaii,

- USA, 2011; 516–524.
18. Brand AJ, Wagenaar JW, Eecen PJ, Holtslag MC. Database of measurements on the Offshore Wind Farm Egmond aan Zee. *Proceedings of the EWEA Annual Meeting*, Copenhagen, Denmark, 2013.
 19. NoordzeeWind BV. Data of the NoordzeeWind monitoring and evaluation programme (NSW-MEP). <http://www.noordzeewind.nl/en/knowledge/reportsdata/> 2013.
 20. Jensen NO. A note on wind generator interaction. *Technical Report Risø-M-2411*, Risø National Laboratory, Roskilde 1984.
 21. Katić I, Højstrup J, Jensen NO. A simple model for cluster efficiency. *Proceedings of the European Wind Energy Association Conference and Exhibition*, Rome, Italy, 1986; 407–410.
 22. Jones E, Oliphant T, Peterson P. Scipy: Open source scientific tools for python. <http://www.scipy.org/> 2001; .
 23. Mueller A. Simplistic minimum spanning tree in numpy. <http://peekaboo-vision.blogspot.com/2012/02/simplistic-minimum-spanning-tree-in.html> Feb 2012; URL <http://peekaboo-vision.blogspot.com/2012/02/simplistic-minimum-spanning-tree-in.html>.
 24. Gill PE, Murray W, Saunders MA. SNOPT: An SQP algorithm for large-scale constrained optimization. *SIAM review* 2005; **47**(1):99–131.
 25. Perez RE, Jansen PW, Martins JRRA. pyOpt: A Python-based object-oriented framework for nonlinear constrained optimization. *Structures and Multidisciplinary Optimization* 2012; **45**(1):101–118, doi:10.1007/s00158-011-0666-3.